Available online at www.sciencedirect.com
SCIENCE DIRECT®
ELSEVIER
Nuclear Instruments and Methods in Physics Research A 515 (2003) 458–466
NUCLEAR INSTRUMENTS & METHODS IN PHYSICS RESEARCH Section A
www.elsevier.com/locate/nima

Energy resolution of a silicon detector with the RX64 ASIC designed for X-ray imaging

D. Bollini[a], A.E. Cabal Rodriguez[b], W. Dąbrowski[c], A. Diaz Garcia[b], M. Gambaccini[d], P. Giubellino[e], P. Grybos[c], M. Idzik[c,e], A. Marzari-Chiesa[f], L.M. Montano[g], F. Prino[h], L. Ramello[h,*], M. Sitta[h], K. Swientek[c], R. Wheadon[e], P. Wiacek[c]

[a] *Dipartimento di Fisica dell'Università di Bologna and INFN, Bologna, Italy*
[b] *CEADEN, Havana, Cuba*
[c] *Faculty of Physics and Nuclear Techniques, Academy of Mining and Metallurgy, Cracow, Poland*
[d] *Dipartimento di Fisica dell'Università di Ferrara and INFN, Ferrara, Italy*
[e] *INFN, Torino, Italy*
[f] *Dipartimento di Fisica Sperimentale dell'Università di Torino and INFN, Torino, Italy*
[g] *CINVESTAV, Mexico City, Mexico*
[h] *Dipartimento di Scienze e Tecnologie Avanzate dell'Università del Piemonte Orientale and INFN, Alessandria, Italy*

Received 6 February 2003; received in revised form 12 June 2003; accepted 9 July 2003

Abstract

Results from a silicon microstrip detector coupled to the RX64 ASIC are presented. The system is capable of single photon counting in digital X-ray imaging, with foreseen applications to dual energy mammography and angiography. The main features of the detecting system are low noise (operation with threshold as low as ≈ 4 keV is possible), good spatial resolution (a pixel of 100 μm × 300 μm when oriented edge-on) and good counting rate capability (up to one million counts per channel with a maximum rate of about 200 kHz per channel). The energy resolution of the system, as obtained with several fluorescence X-ray lines, is described.

PACS: 87.57.−s; 07.50.Qx; 29.40.Gx; 29.30.Kv

Keywords: Medical imaging; X-ray detection; Silicon Strip Detectors; Front-end electronics; X-ray spectroscopy

1. Introduction

There is currently widespread interest in developing digital X-ray imaging with silicon detectors. For specific diagnostic applications, such as mammography, the dual energy technique makes it possible to isolate materials of specific interest via the energy subtraction method: after early theoretical developments [1,2] by Macovski and

*Corresponding author. Address for correspondence: Dipartimento di Scienze e Tecnologie Avanzate, Università del Piemonte Orientale, Corso Borsalino 54, I-15100 Alessandria, Italy. Tel.: +39-011-6707372; fax: +39-011-6699579.
E-mail address: ramello@to.infn.it (L. Ramello).

0168-9002/$ - see front matter © 2003 Elsevier B.V. All rights reserved.
doi:10.1016/j.nima.2003.07.020

co-workers, several authors investigated the application of dual energy imaging [3,4]. However, the clinical application has been so far limited by the broad energy spectrum of conventional X-ray sources (with the exception of synchrotron radiation, which however is available only in a few locations). Recently a quasi-monochromatic X-ray source [5] based on an array of mosaic crystals has been developed and further work towards a dichromatic X-ray source is being carried out [6]. Coupling a silicon detector with single photon counting capability to a dichromatic X-ray beam has the advantage of reducing the dose to the patient (with respect to traditional screen/film combination) without losing in image definition. Of course the efficiency for converting X-rays (via the photoelectric effect) must be high enough and this can be achieved by orienting the detecting elements (microstrips in our case) parallel to the incoming beam; in this configuration a two dimensional image can be obtained by scanning. The energy information can be obtained either by making two scans with two identical detectors set at different thresholds, or better by implementing a double threshold scheme in the front-end electronics. In both cases, a very simple and practical readout is obtained with counters connected to each amplification/discrimination channel.

In this paper we report on systematic tests of a detecting system built around a silicon AC-coupled microstrip detector and the RX64 ASIC, which is derived from the previous RX32 and COUNT32 ASICs [7]. Two prototypes, the first with 128 and the second with 384 channels, were built and tested both with radioactive sources and with an ordinary (wide band) X-ray beam. The system is intended to be used in scanning mode to obtain two-dimensional images with dichromatic X-ray beams. In the present version of the RX64 ASIC a single threshold is implemented; a double threshold version is in preparation.[1]

[1] First tests of the RX64-DT ASIC, obtained in March 2003 [8], indicate a 30% increase of the noise with respect to the single threshold version, which is attributed both to the shorter shaping time chosen and to the increased temperature of ASIC and detector. Peltier cooling is being considered in order to alleviate this problem. The counting rate capability is the same of the single threshold version, see Table 2.

2. Microstrip detectors

The range of useful X-ray energies for mammography and other applications, like angiography at the iodine K-edge, goes up to about 40 keV. A silicon detector of standard 300 μm thickness has a quickly decreasing conversion efficiency in this range, reaching 3.5% at 40 keV (considering only the photoelectric effect); for this reason, several authors have proposed to increase the efficiency with the edge-on orientation. In order to maintain a good noise performance, both the capacitance and the leakage current per strip must be kept as low as possible. A practical limit for our electronics (see next section) is 5 pF and 100 pA, respectively.

Keeping this in mind, we have chosen (see Table 1) an AC-coupled detector with rather short strips (1 cm); the pitch of 100 μm gives us a pixel size of $100 \times 300\ \mu m^2$ which seems reasonable when compared to the size of the details which have to be detected in angiography (approximately 0.4 mm), while for microcalcifications in mammography a smaller pixel size of $100 \times 100\ \mu m^2$ can be obtained by collimation.

For the first prototype we have used a 132-strip detector with FOXFET biasing,[2] while for the second prototype a 400-strip detector has been used. Both prototypes had identical strip length (10 mm) and pitch (100 μm) resulting in a total geometrical strip capacitance of about 2 pF.

A photograph of the detector's corner is shown in Fig. 1, where the first 15 strips, the bias line, the guard ring and the physical edge of the detector are visible.

Detectors have been characterized with I–V and C–V measurements under a semiautomatic Alessi probe station REL 4500: I–V measurements were obtained with the Hewlett Packard semiconductor parameter analyzer 4145B and C–V measurements with the Hewlett Packard precision LCR meter 4284A, while the data acquisition and analysis software was developed with LabVIEW 6.0. A typical C–V curve for a group of four contiguous strips is shown in Fig. 2. The full depletion voltage

[2] Detectors were designed and fabricated by ITC-IRST, Trento, Italy.

Table 1
Summary of the main electrical parameters measured on the microstrip detectors

Parameter	Value
Strip length	10 mm
Thickness	300 μm
Dead region (Si, edge-on config.)	765 μm
Strip pitch	100 μm
Number of channels	132 (400)
Depletion voltage	≈25 V
Leakage current per strip at full depletion	≈50 pA

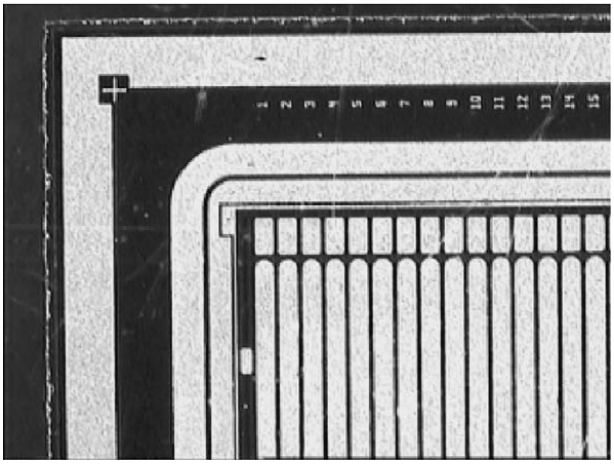

Fig. 1. Detector's corner.

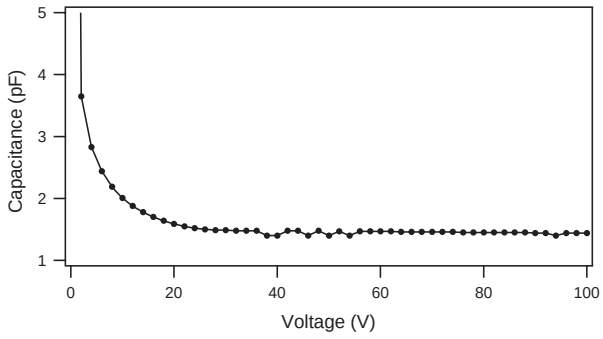

Fig. 2. *C–V* curve for a group of four contiguous strips.

was in the range 23–26 V both for 132 and 400 strip detectors. In order to ensure good charge collection efficiency, the normal operating voltage was set at 60 V, well above the full depletion voltage.

The measured leakage current per strip at 60 V bias was ≈50 pA (at $t = 23^{\circ}C$) for 132-strip detectors, with only a very few strips showing larger (up to ≈3 nA) currents. In Fig. 3 a typical distribution of strip currents for a 132-strip detector is shown. The 400-strip detectors presented an average leakage current per strip of 44 pA at 60 V bias voltage (measurement done at $t = 25^{\circ}C$); the RMS deviation among 10 measured detectors was about 5%. The current collected by the guard ring was between 4% and 6% of the total current flowing through the 400 strips. Results presented in the following sections concern both the first (132 strip) and the second (400 strip) prototype. The 132-strip detector was operated at 60 V bias voltage, while with the second prototype data at 60 and 100 V bias voltage have been collected.

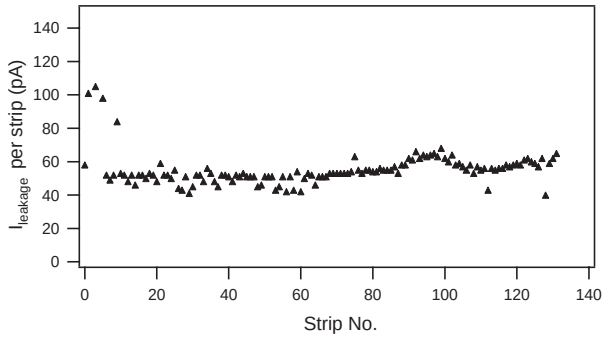

Fig. 3. Leakage current for the 132 strips of a detector at 60 V.

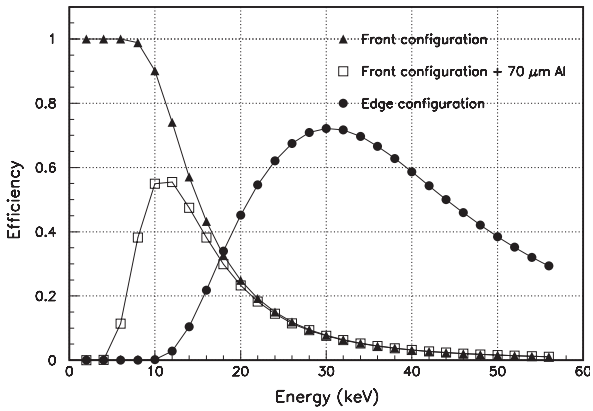

Fig. 4. Theoretical quantum efficiency in front and edge-on configurations vs. photon energy.

Calculations of the expected quantum efficiency for photoelectric conversion in our detector in the "front" configuration and "edge-on" configurations are presented in Fig. 4. The quantum efficiency for photoelectric conversion in the silicon layer of 300 μm thickness has a maximum value of about 55% at 10–12 keV (including 70 μm of Al used as a light shield) and then decreases quickly with increasing energy. In the edge-on configuration, taking into account the dead layer of 765 μm silicon, the quantum efficiency is always higher for energies above 18 keV.

3. The RX64 binary readout ASIC

Our readout electronics are based on the so-called binary architecture, in which each channel of the front-end provides 1-bit yes/no information in response to the signal generated beneath a given detector strip. Binary information can be easily stored in the integrated circuit separately for each channel, which allows the system to work with high rates of incoming X-rays. The block diagram of the complete RX64 IC is shown in Fig. 5. The chip comprises five basic blocks: analogue front-end channels, counters, input–output block, control block and calibration circuit containing digital to analogue converters (DACs). Each of the analogue front-end channels is composed of a preamplifier, a shaper and a comparator which provides discrimination of the analogue signal at a given level. The feedback resistances of the preamplifier and shaper blocks are tunable by means of dedicated DACs which are used to tune the preamplifier decay time and the shaper peaking time. These settings influence also the noise and the gain of the circuit; in particular short shaping times imply low gain, while the preamplifier feedback resistor value affects the noise level and the maximum sustainable rate.

Due to the statistical nature of X-ray sources the signals at the output of the discriminator appear completely randomly in time and are stored in 20-bit asynchronous counters. The counters are grouped in blocks of eight channels each and the data from each block can be read out through tristate outputs.

In a single chip we have integrated 64 channels which can simultaneously process signals and store data from 64 elements of a silicon strip detector. Such architecture provides fully parallel signal processing, including data storage, from all strips. It is suitable for high counting rate applications since the amount of data to be handled is minimized already in the front-end part [9,10]. The counting rate of the system is determined by

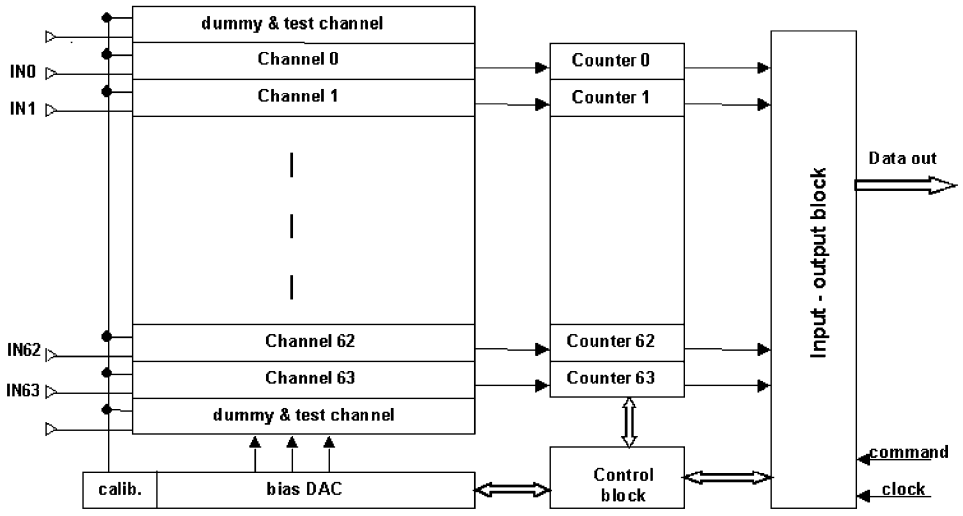

Fig. 5. Block diagram of the RX64 chip.

the pile-up effects in the analogue part of the ASIC, and is on the level of 200 kHz [7]. In addition to the basic functions which control the data storage and readout the control block provides the settings of the DACs which are used in the front-end block to bias the analogue circuits and to control the internal calibration circuit.

The chip is controlled by commands delivered from an external controller through a serial link. The control block receives the commands, decodes them and executes them by sending the control signals and data to the other blocks.

The signal-to-noise ratio is one of the most critical issues for the RX64 performance. Sufficient separation between the noise level and the signal level is required to provide high detection efficiency and limited noise count rate. In order to make a multichannel system practical for use with a single global threshold, a good matching of the gain and offset for all channels is required. The detailed description of the RX64 can be found in Ref. [11], while the main measured parameters of RX64 chip are summarized in Table 2.

Table 2
Main parameters of the RX64 ASIC

Parameter	Measured value
Gain (dep. on peaking time)	60–105 μV/electron
ENC (Cdet = 2.5 pF, Idet = 100 pA, Tpeak = 0.7 μs)	167 el. rms
Input range	up to 12,000 el.
Peaking time	0.5–1.0 μs
Counting rate	200 kHz/channel
Power consumption	2.5 mW/channel

4. Energy resolution results

We report in this section results on linearity, noise and energy resolution obtained with two prototypes. The first prototype, consisting of a 132 strip detector directly connected to a couple of RX64 ASICs, has 128 equipped channels (see Fig. 6). The second prototype was built using a 400 strip detector and six RX64 chips, for a total of 384 equipped channels; in this case the connection between strips and preamplifiers was made through a pitch-adapter (Al strips on glass substrate) developed for this application.

In order to reach the relatively high energies, up to 40 keV, foreseen for double energy mammography [12] (18 and 36 keV, or 20 and 40 keV) and angiography (around the iodine K-edge at $\sim$33 keV), a relatively short shaping time of 0.5 μs, implying a low gain (see previous section), was chosen for both prototypes.

A preliminary study of the system's linearity and noise was made using the internal calibration feature of the RX64 chips. In this case, test charges of up to $\approx 10,000$ electrons were injected into each preamplifier (through integrated capacitors of nominal value 75 fF), allowing us to establish the

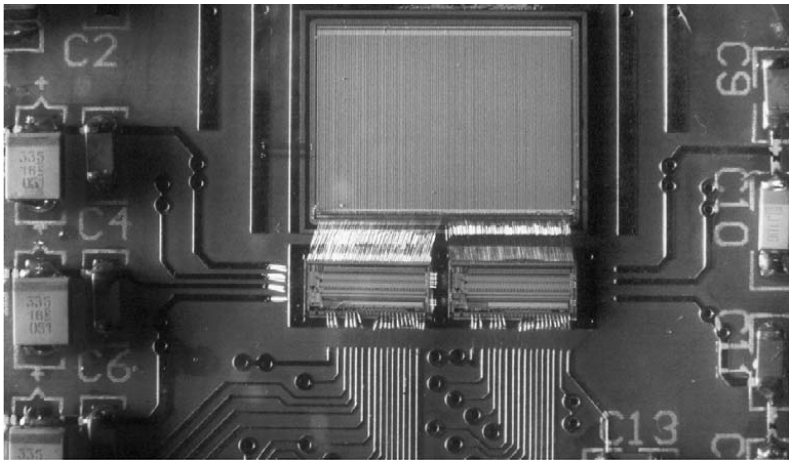

Fig. 6. Photograph of the board with 132-strip detector and two RX64 ASICs.

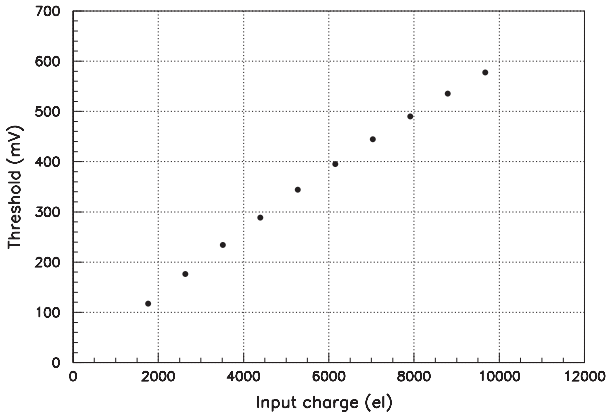

Fig. 7. Linearity of the amplifier and shaper part of the RX64 chip.

linearity range (i.e. the input charge region where the response of the front-end is linear) of the system and the values of gain, offset and noise for each channel. Threshold scans, where the number of pulses exceeding the varying comparator threshold are recorded, allowed us to obtain integral pulse height spectra and, upon differentiation, differential spectra, which were then fitted by a Gaussian function. The linearity range of the system extended to about 6000–6500 electrons ($\approx$20–22 keV), as presented in Fig. 7, which refers to a single channel of the 128-channel prototype. With the peaking time of 0.5 μs, average measured values were 62 μV/el. for the gain (using the nominal value for the injecting capacitor) and 131 el. RMS for the noise; the comparator offset was small and its RMS variation was about one half of the noise. With the 384-channel prototype, we measured an average gain of 64 μV/el. and a noise of 165 el. RMS. The higher noise of the 384-channel prototype is due in part to the addition of the pitch adapter and in part to the layout of the board with six ASIC's. By modifying the preamplifier feedback resistor and the detector bias voltage, the noise for the 384-channel was then reduced to 141 el. RMS. Including the saturation of gain which was observed for high values of injected charge, we expect that the upper limit of the discriminator threshold (630 mV) corresponds to $\approx$40 keV.

The energy resolution of the system was then measured by making threshold scans with two X-ray setups: a compact ^{241}Am fluorescence source and a larger fluorescence setup including an X-ray tube. Measurements were taken with both prototypes, giving very similar results: here only the measurements taken with the 384-channel prototype are reported in detail. The source setup included a 370 MBq ^{241}Am source with six different fluorescence targets, of which we used the Cu, Rb, Mo, Ag and Ba ones, covering the energy range between 8.05 and 32.2 keV. Data collection times were of the order of 1000–1500 s per threshold in order to obtain $\approx$1000 counts for the most external strips. Such a long measurement time was imposed by the low flux of X-rays from the fluorescence source.

The tube fluorescence setup included a Cu-anode X-ray tube[3] which works in the range 10–60 kV and delivers up to 60 mA at 30 kV (up to 33 mA at 60 kV). We have used the tube with a point focus of 1.0×1.0 mm^2, without filter (in this case, the 0.4 mm Be window gives $\geqslant$93% transmission for the Cu K_α line). The target was placed very close to the tube ($\approx$2 cm) and the detector was placed at 90° with respect to the beam line, at 11 cm distance from the target with the strips oriented orthogonally to the beam axis (front configuration). A 0.8 mm wide lead collimator was placed between the target and the detector, 4.5 cm upstream from the detector. Five target materials were used, namely Cu ($K_\alpha = 8.04$ keV), Ge ($K_\alpha = 9.88$ keV), Mo ($K_\alpha = 17.4$ keV), Ag ($K_\alpha = 22.1$ keV) and Sn ($K_\alpha = 25.3$ keV). The data collection time was 3 s per threshold for a given target in order to obtain $\approx$7000–10,000 counts per strip.

The differential spectra collected with both the source (Rb, Mo and Ag targets) and the tube (Cu, Ge, Mo, Ag and Sn targets) fluorescence setups are presented in Fig. 8 for a typical channel; the horizontal axis is expressed in discriminator threshold units (mV). With this detector we performed a further optimization of the operating parameters. The detector was operated at 100 V bias voltage, and the preamplifier feedback resistor was optimized so as to minimize the noise. We note the good energy resolution of the system, as

[3] Model KFNCu4K from Siemens AG, Germany.

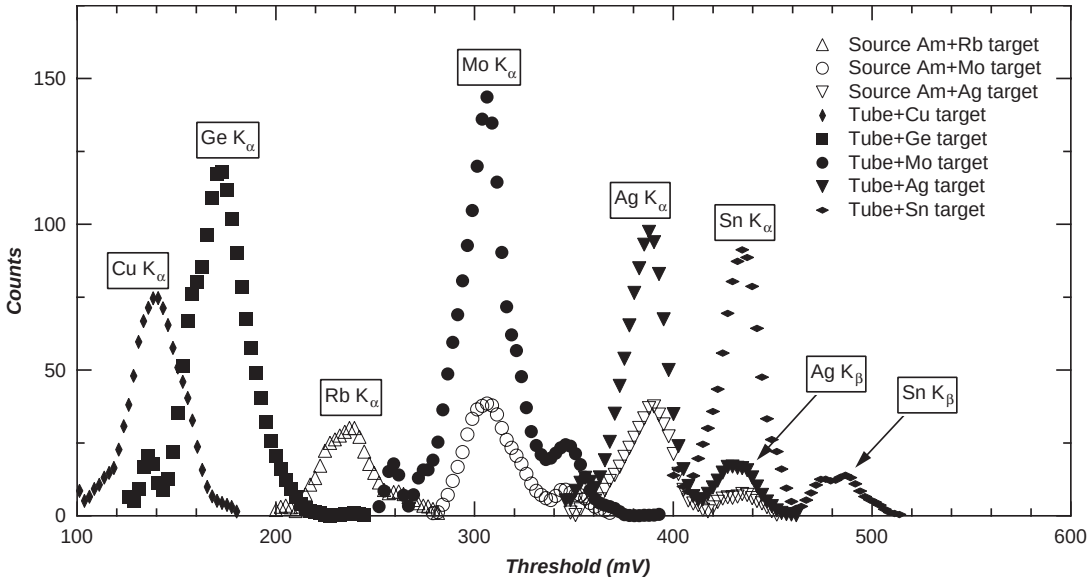

Fig. 8. Fluorescence spectra recorded with the 400 strip detector at 100 V bias voltage using the Am source and the X-ray tube. Counts for the X-ray tube data are downscaled by a factor of 2.

demonstrated by the K_β peaks clearly visible for the Ag and Sn targets. Also, there is excellent agreement between the Mo and Ag target spectra obtained with both methods.

Performing a Gaussian fit to the spectra of Fig. 8 we have obtained the peak centroids corresponding to the X-ray emission lines of the various targets; Fig. 9 presents the peak centroids as a function of energy, demonstrating a good linearity up to 25 keV. The computed gain for the particular channel of Fig. 9 operated at 100 V obtained from a linear fit to the Rb, Mo and Ag data points is 17.4 mV/keV. The average among all the 384 channels gives 17.5 ± 0.4 mV/keV, which translates into 63.5 μV/electron (3.63 eV per e–h pair in silicon) in good agreement with the one found with the internal calibration which however suffers from the uncertainty on the 75 fF capacitance value. Furthermore, the saturation of gain already observed with internal calibration was confirmed with measurements taken with the Sn and Ba target (the latter one, at 32.2 keV energy, is not shown in Figs. 8 and 9).

The width of the Gaussian peak has been estimated for the Ag target, for which the K_α and K_β peaks are well separated. With the 132 strip detector we obtain an average Gaussian

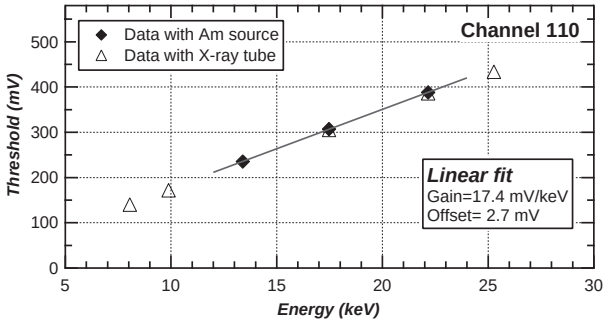

Fig. 9. Discriminator threshold values vs. energy for a single channel obtained using the Am source and the X-ray tube. Detector operated at 100 V.

width of the Ag K_α peak of 11.22 mV ($\approx$0.66 keV), corresponding to an ENC of 180 el. RMS. With the 400 strip detector (see Fig. 8) we obtain the ENC values of 185 el. RMS using the Am source and the Ag target. A very similar value (186 el.) is obtained with the X-ray tube setup.

We have also performed, with the 400-strip prototype, a study of the gain and noise variation with the detector bias voltage. Comparing the situation at 40, 60, 80 and 100 V, we found a slight increase of the Ag peak value with increasing bias voltage, together with a reduction of the peak width. With respect to the normal operating bias

voltage of 60 V, we measured a 2% increase of the peak value and a 3.5% decrease of the width, for operation at 100 V.

In the low noise configuration obtained by increasing the preamplifier feedback resistor and the detector bias voltage, values of 154 (151) electrons are obtained for the width of the Ag K_α peak in the Am source (X-ray tube) setup. The values of the Gaussian widths obtained for the 128 channel and 384 channel detectors with the internal calibration and with the Ag fluorescence target are summarized in Table 3. It can be seen that in the same working conditions the noise is higher for the 384 channel system and furthermore that the noise performance can be significantly improved by optimizing the bias voltage and the preamplifier feedback resistor.

The above results were obtained with the detector in "front" configuration, i.e. with strips approximately orthogonal to the incident X-rays. As explained in Section 2, in order to obtain higher efficiency in the energy range of 18–40 KeV of the intended imaging applications it is necessary to adopt the "edge-on" configuration (strips parallel to incident X-rays). Quasi-monochromatic X-ray beams [6] will be crucial to verify the performance of our system, in particular its efficiency as a function of energy and its rate capability, in conditions which will be very close to the final application. Preliminary results obtained with the "edge-on" configuration have been reported in Refs. [8,13,14], which confirm the expected increase of efficiency indicated in Fig. 4.

Table 3
Average width of the Gaussian peaks expressed in ENC for the 128 channel and 384 channel detectors for different values of preamplifier feedback resistor (R_{fed}) and detector bias voltage

	ENC 128-*chan.*	ENC 384-*chan.*	
	Low R_{fed} 60 V bias	Low R_{fed} 60 V bias	High R_{fed} 100 V bias
Internal calibration	131	165	141
Source + target			
Am + Ag	180	185	154
Tube + Ag	—	186	151

5. Conclusions

We have obtained first results concerning the energy resolution of a single photon counting system based on silicon microstrip detectors of 100 μm pitch and on the low noise RX64 ASIC. Using fluorescence X-rays, a measured ENC of 185(154) electrons RMS has been obtained with the larger prototype (400 strips, of which 384 were equipped) at 22.1 keV energy. The system is well suited for dual-energy operation in the range of interest for angiography and mammography, provided it is oriented "edge-on" in order to reach a good quantum efficiency. More tests are foreseen with quasi-monochromatic X-ray beams, and an improved system with double threshold ASIC's is in preparation.

Acknowledgements

We are grateful to B. Pini for help with the assembly of detectors and ASICs, to E. Filoni for the layout of the pitch adapter, and to F. Rotondo for help with cabling. We acknowledge help from L. Fava, P.F. Ottria and D. Panzieri for setting up the X-ray tube in the Physics Laboratory of the Dipartimento di Scienze e Tecnologie Avanzate in Alessandria. This work was supported by the Ministero dell'Università e Ricerca Scientifica e Tecnologica (MURST) of Italy under contract N. COFIN-2000-MM02095297-003. We are grateful to the Istituto Nazionale di Fisica Nucleare (INFN)—Sezione di Torino for financial and logistic support. Two of us (A.E.C.R., A.D.C.) acknowledge the support from the ICTP Programme for training and research in italian laboratories (ICTP-TRIL).

References

[1] R.E. Alvarez, A. Macovski, Phys. Med. Biol. 21 (1976) 733.
[2] L.A. Lehmann, R.E. Alvarez, A. Macovski, W.R. Brody, Med. Phys. 8 (1981) 659.
[3] P.C. Johns, D.J. Drost, M.J. Yaffe, A. Fenster, Med. Phys. 12 (1985) 297.
[4] B.K. Stewart, H.K. Huang, Med. Phys. 17 (1990) 866.

[5] M. Gambaccini, et al., Nucl. Instr. and Meth. A 365 (1995) 248.
[6] M. Gambaccini, et al., SPIE Proc. 3770 (1999) 174.
[7] P. Grybos, W. Dabrowski, IEEE Trans. Nucl. Sci. NS-48 (3) (2001) 466.
[8] L. Ramello, et al., Results about imaging with silicon strips for angiography and mammography, Presented at the VII Mexican Symposium on Medical Physics, Mexico City, March 26–26, 2003, AIP Proceedings, to appear.
[9] G. Comes, et al., Nucl. Instr. and Meth. A 377 (1996) 440.
[10] W. Dabrowski, et al., Nucl. Instr. and Meth. A 421 (1999) 303.
[11] P. Grybos, et al., Microelectron. Reliab. 42 (2002) 427.
[12] A. Tuffanelli, et al., SPIE Proc. 4682 (2002) 21.
[13] F. Prino, et al., A silicon strip detector coupled to the RX64 ASIC for X-ray diagnostic imaging, Presented at RESMDD02 conference, Firenze, July 2002, Nucl. Instr. and Meth. A, (2003) to appear.
[14] L. Ramello, et al., X-ray imaging with a silicon microstrip detector coupled to the RX64 ASIC, Presented at IWORID02 conference, Amsterdam, September 2002, Nucl. Instr. and Meth. A 509 (2003) 315.